

DETECTING SEISMIC AIRGUN SHOTS IN THE MARGINAL ICE ZONE SOUNDSCAPE

F Geyer Nansen Environmental and Remote Sensing Center, Bergen, Norway

1 INTRODUCTION

Acoustic experiments using an integrated ice station were carried out during August 2012 and September 2013 in the Marginal Ice Zone of Fram Strait between Greenland and Svalbard as part of the UNCER-ICE and WIFAR research projects. Data from the two four-day experiments were used to identify and quantify different soundscape components in the Marginal Ice Zone. This study was published in JASA by Geyer et al. (2016)¹. Among the studied soundscape components were components due to natural noise sources such as ice noises and marine mammal vocalizations. Other soundscape components were anthropogenic, such as seismic airgun noise from distant sources or ship cavitation noise from the research icebreaker employed in the fieldwork. Both of these anthropogenic noise types were characterized by their regularly pulsating nature. Especially the seismic airgun noise consisted of series of regularly repeated shots. Such a series of shots, e.g. occurring every 8 seconds, would last for half an hour or longer before a break in the seismic shooting would appear or the time distance between shots would change. This new time distance between shots would then again be kept constant for half an hour or more. This characteristic regularity of seismic airgun noise was used to detect this type of noise and to separate and quantify its contribution to the observed soundscape.

The technique employed to do this was to calculate power spectrums of acoustic spectrograms, i.e. to calculate power spectra of the noise level time series at each sound frequency as identified by the acoustic spectrogram. While this technique and its main results are presented in Geyer et al. (2016)¹ we want to present its usefulness here in greater detail. This is done both by presenting its application on the Marginal Ice Zone acoustic observations described above and by presenting idealized time series of background noise and seismic airgun noise, which illustrate the capabilities and limitations of this method.

2 ANALYSIS OF SEISMIC AIRGUN NOISE IN THE MARGINAL ICE ZONE

2.1 Using power spectra of acoustic spectrograms to detect seismic airgun noise

Many man-made noises are either noises occurring at a constant frequency, e.g., the engine noise from a ship travelling at constant speed, or regularly pulsating noises, such as a series of seismic airgun shots. Airgun shots observed in Fram Strait occurred typically every 8-15 seconds, depending on the purpose of the seismic survey and the water depth in which the seismic exploration vessel is operating. This characteristic regularity of seismic airgun noise can be used to detect this type of noise and to separate and quantify its contribution to the observed soundscape. For this purpose a spectral analysis of the acoustic spectrograms was carried out.

Acoustic spectrograms consist of time series of sound levels as a function of frequency. The spectrograms used here to study seismic airgun noise have a frequency resolution of 3.81 Hz and a time resolution of 0.131 s. For the following analysis the data were binned into 1/10 octave frequency bands to reduce the amount of data. Power spectra were then calculated for time series at each sound frequency for hourly recording intervals, averaging over 50% overlapping (detrended) Kaiser windows with a window length of 2048 samples. The new power spectra are a function of

frequency bands (sound frequency) and modulation frequency, which describes the amplitude modulation of sound at a given frequency band. The power spectra can be presented as contour plots as shown in the lower panel of Fig. 1. The modulation frequency describes the variability of sound levels at a given frequency with time and can be used to identify sounds with a periodic pattern (e.g., repeated airgun shots). A continuous wave sound (e.g., ship engine noise) will have a modulation frequency close to 0 Hz.

The upper panel of Figure 1 presents an example of a spectrogram of one-hour duration. The spectrogram contains seismic airgun noise, marine mammal vocalisations and ship engine noise. The different noise types are marked in the spectrogram. The lower panel of Figure 1 shows the resulting power spectrum of the spectrogram. Natural sounds, such as marine mammal noises (in this case *Balaena mysticetus* calls), with their irregular time variation form wide horizontal bands. Seismic airgun noise is visible as vertical bars at 15-110 Hz acoustic frequency. The bar with the lowest modulation frequency identifies the shooting interval of the seismic exploration, while bars at higher modulation frequencies represent the harmonics. Ship engine noise with its slowly varying amplitude and narrow frequency band is observed as a point at 330 Hz sound frequency close to 0 Hz modulation frequency. The weak marine mammal noises in this example are visible as horizontal bands of increased power at 130-300 Hz acoustic frequency. The example shown in Figure 1 displays strong seismic noise and weak marine mammal noises. Figure 2 present the case of strong marine mammal noise, with no seismic noise present. Here the horizontal bands from the marine mammal noise dominate; the vertical bar signifying seismic noise is absent. In case which combine the two noise sources the seismic signal would still clearly identifiable due to its sharp signature in modulation frequency stemming from the precise timing of the repeating seismic airgun shots.

Power spectral densities of hourly spectrograms were calculated for the 2012 and 2013 experiments using a window length of 2048 samples as described above. Inspecting the power spectra showed seismic noise as a clear peak at modulation frequencies between 8-13 s (the repetition time of successive airgun shots) at sound frequencies of 15-120 Hz. The strongest signal occurred at 40 Hz sound frequency. The analysis presented here allowed the detection of even weak seismic signals and the precise determination of the sound frequencies influenced by the seismic airgun noise. Directly using the regular shooting intervals that characterize seismic airgun noise gives a high signal-to-noise ratio for seismic airgun noise vs. the other noise contributing to the soundscape at the same sound frequencies as the seismic airgun noise.

While the signature of seismic airgun noise and marine mammal vocalizations is strongly pronounced in the spectrograms and power spectra of acoustic spectrograms, their influence on hourly mean noise levels and standard deviation of noise levels are much smaller. Mean noise levels and standard deviation of noise levels for hours 72 and 76 of the 2012 experiment are presented in Figures 4 and 5, respectively. Because noise levels distribution were found to be roughly Gaussian in dB, both mean levels and standard deviations were here calculated in dB. The seismic airgun noise is visible as a small increase in mean hourly noise levels between 20 Hz and 120 Hz (Figure 4, left panel). It does have any visible impact on the standard deviation (Figure 4, right panel). Marine mammal vocalizations on the other hand have a very small impact on the mean noise levels (Figure 4+5, left panel), but increase the standard deviation of noise levels. This is especially pronounced for the case of strong marine mammal vocalizations as they occurred during hour 76 of the 2012 experiment (Figure 5, right panel).

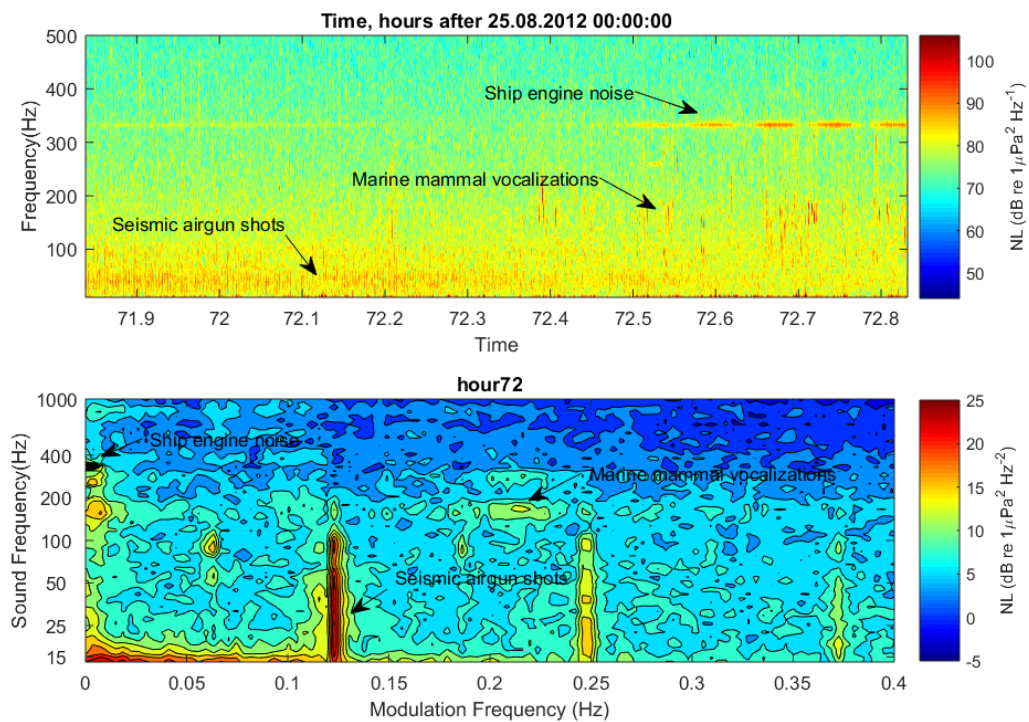


Figure 1: Spectrogram (upper panel) and modulation frequency analysis (lower panel) identifying seismic airgun shots at 15-120 Hz sound frequency approximately every 8 seconds, hour 72 of the 2012 experiment (from Geyer et al., 2016)¹.

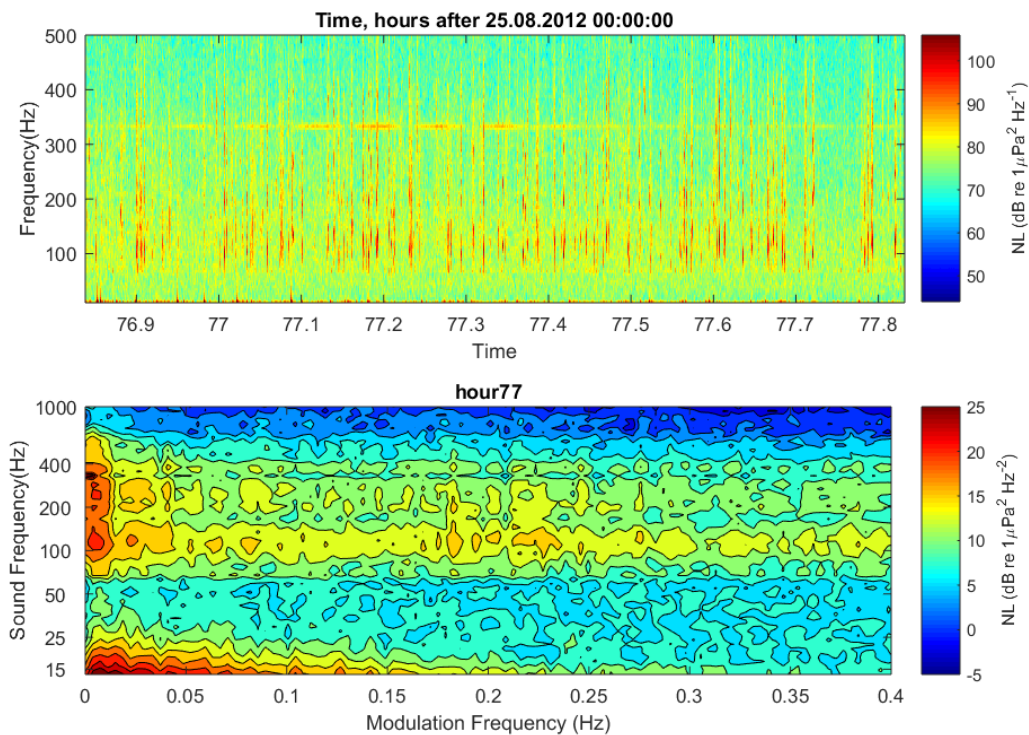


Figure 2: Spectrogram (upper panel) and modulation frequency analysis (lower panel) displaying strong marine mammal vocalizations at 70-800 Hz sound frequency with an irregular time distribution, seismic airgun noise is absent. Hour 76 of the 2012 experiment.

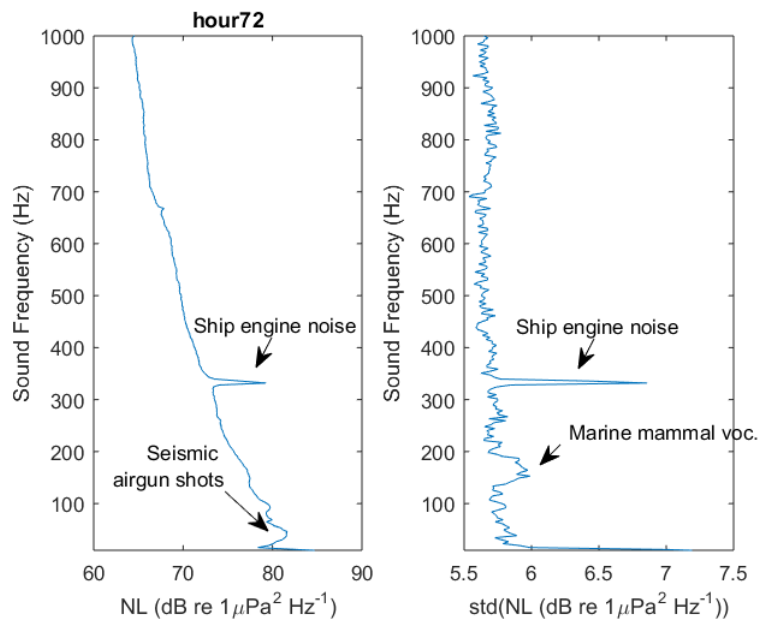


Figure 3: Mean noise level as a function of frequency and standard deviation of noise level (both calculated in dB) for hour 72 of the 2012 experiment.

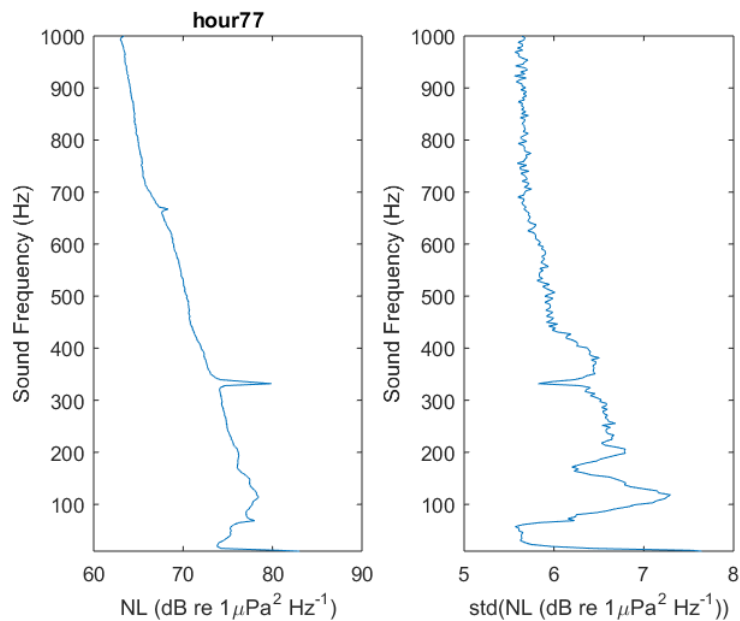


Figure 4: Mean noise level as a function of frequency and standard deviation of noise level (both calculated in dB) for hour 76 of the 2012 experiment.

2.2 Simulations of idealized seismic airgun noise

To test the efficiency and limits of the seismic airgun noise detection, three simple idealized experiments were carried out. Background noise levels were set to correspond to the values documented in Figures 4 and 5, simplified to a linear noise level spectrum reaching from 65 dB at 1000 Hz to 81 dB at 0 Hz. For the first idealized experiment the background signal was varied by Gaussian noise with 6 dB standard deviation, to simulate the variability of the background noise as documented in Figures 4 and 5. The seismic airgun signal was simulated as a series of 4 dB triangular peaks of 3 seconds width repeating every 5 seconds for acoustic frequencies up to 120 Hz. These peaks were simply superimposed on the background noise field. This results in the mean noise level functions and standard deviations as displayed in Figure 5. The spectrogram of the simulated signal (Figure 6, upper panel) shows a moderately strong series of seismic airgun pulses overlaying a noisy background field, comparable to the situation in Figure 1. The power spectrum of the spectrogram clearly identifies the pulsating seismic signal at a modulation frequency of 0.125 Hz, corresponding to the shooting interval of 8 seconds. The signals identified at 0.25 Hz and 0.375 Hz modulation frequency are the first and second harmonics of the triangular pulse signal. Replacing the triangular pulses with a sinus modulation would eliminate the harmonics. Replacing the triangular pulses with a series of infinitely narrow pulses (a Dirac comb) would result in all harmonics having equal strength. In the same manner, a widening of the triangular pulses leads to a weakening of the higher harmonics, while a narrowing of the pulses strengthens them.

The idealized seismic signal and the noisy background were varied in a series of experiments to illustrate the sensitivity of the method. Figure 7 shows results from the second idealized experiment. In this experiment the simulated seismic airgun shot series of the same shape as described above, but with a strength of only 2 dB above the background noise (half the strength of the first experiment). The background noise and its variability was kept identical to the first experiment. The seismic signal is still clearly visible at 0.125 Hz modulation frequency and 15-120 Hz sound frequency (Figure 7, lower panel). The second harmonic of the seismic signal, however, has become nearly indistinguishable from the background. If we were to reduce the strength of the seismic airgun noise further to 1 dB above the background, it would just be barely identifiable in the power spectrum of the acoustic spectrogram in this idealized experiment setup (not shown).

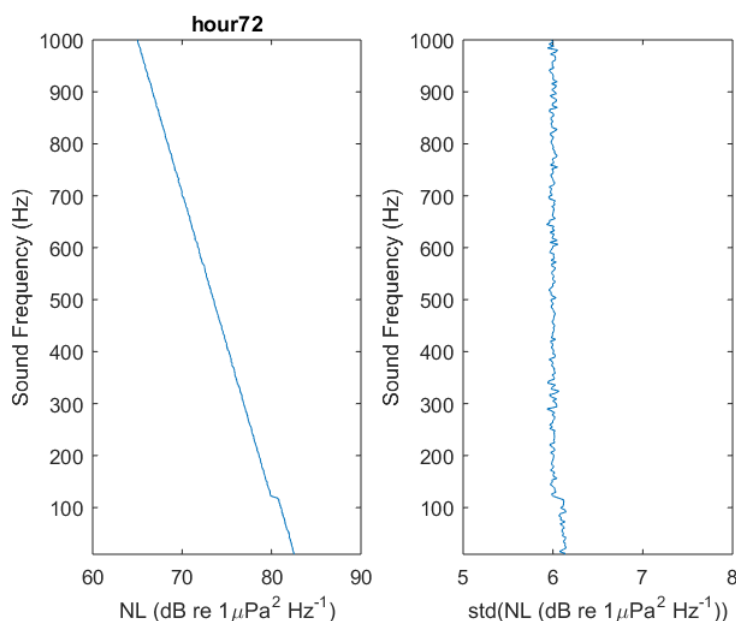


Figure 5: Mean noise level as a function of frequency and standard deviation of noise level (both calculated in dB) for the first idealized experiment: mean background noise increasing linearly from 65 dB at 1000 Hz to 81 dB at 0 Hz, background noise varied Gaussian with a standard deviation of 6 dB, seismic signal 4 dB above background levels for 0 Hz to 110 Hz sound frequency.

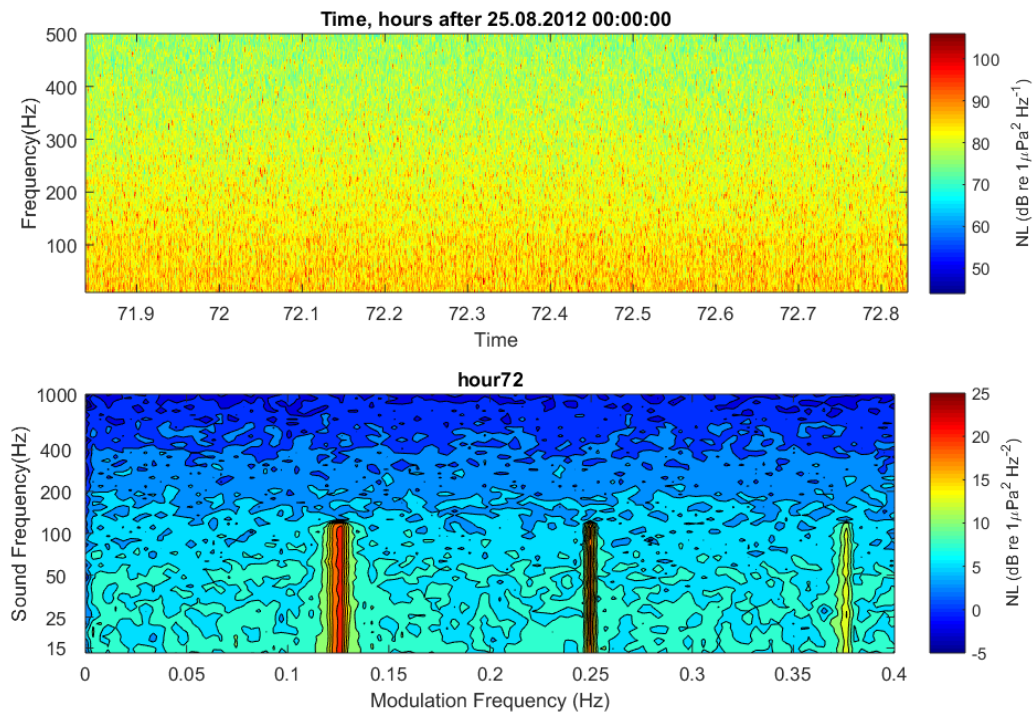


Figure 6: Spectrogram (upper panel) and modulation frequency analysis (lower panel) from first idealized experiment: mean background noise increasing linearly from 65 dB at 1000 Hz to 81 dB at 0 Hz, background noise varied Gaussian with a standard deviation of 6 dB, seismic signal 4 dB above background levels (0-100 Hz sound frequency).

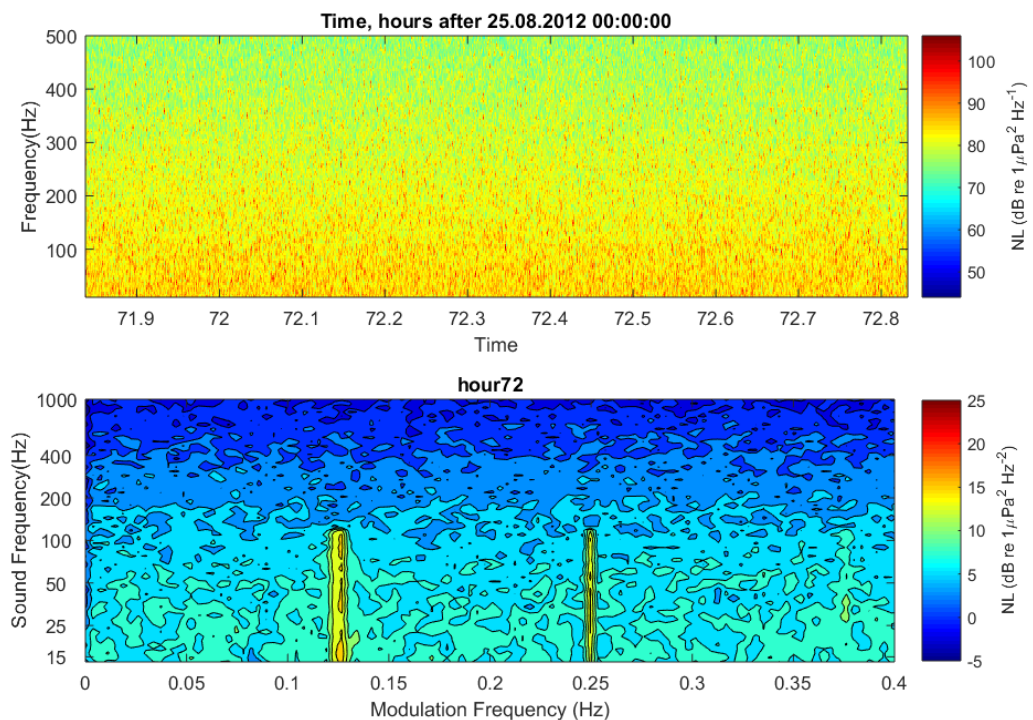


Figure 7: Spectrogram (upper panel) and modulation frequency analysis (lower panel) from second idealized experiment: mean background noise increasing linearly from 65 dB at 1000 Hz to 81 dB at 0 Hz, background noise varied Gaussian with a standard deviation of 6 dB, seismic signal 2 dB above background levels (0-100 Hz sound frequency).

In the third idealized experiment, the background variability was increased, simulating e.g. the presence of stronger marine mammal vocalizations or in general a noisier natural environment. Figure 8 displays the results from this third experiment: the standard deviation of the background is doubled to 12 dB from the original 6 dB, while the seismic signal is held at 4 dB above the background. The effect of doubling the background variability is very similar to the second experiment, where the seismic signal strength was halved: the signal is still clearly identifiable while the second harmonic starts to melt into the background. Reducing the seismic signal from 4 dB above background to 2 dB above background in the third experiment would make the seismic signal just barely discernible in the plotted power spectrum of the acoustic spectrogram. Thus, the limit for identifying the seismic signal is 1 dB above background with a background standard deviation of 6 dB, and 2 dB above background for a background standard deviation of 12 dB using the power spectrum of acoustic spectrogram method in the presented idealized setup.

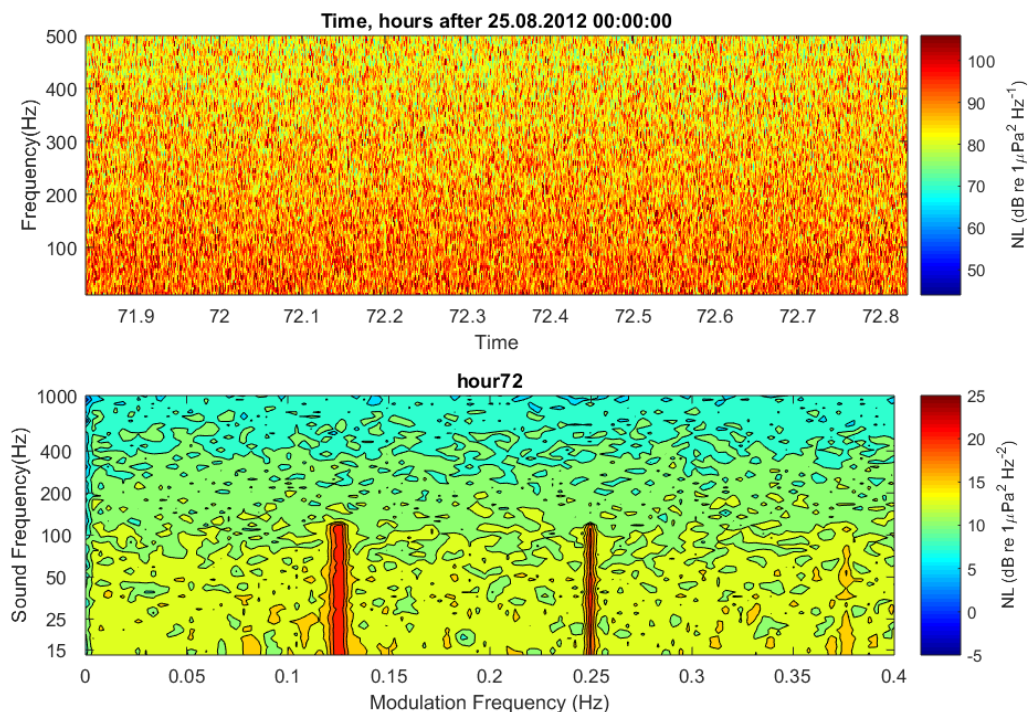


Figure 8: Spectrogram (upper panel) and modulation frequency analysis (lower panel) from first idealized experiment: mean background noise increasing linearly from 65 dB at 1000 Hz to 81 dB at 0 Hz, background noise varied Gaussian with a standard deviation of 12 dB, seismic signal 4 dB above background levels (0-100 Hz sound frequency).

3 CONCLUSIONS

Power spectra of spectrograms are a fast and efficient way to search for pulsating signal, which are not a priori known. All that is needed is a rough idea about the approximate ranges of sound frequency and modulation frequency (or pulsation period) to choose appropriate parameters for the calculation of the power spectra. Without further processing, power spectra of spectrograms provided a fast visual way to detect the presence of seismic airgun shots in the Marginal Ice Zone dataset analysed in Geyer et al. (2016)¹. With further processing it is possible to make use of the increased signal-to-noise ratio of pulsating signals after in the power spectra. One possible avenue was presented in Geyer et al. (2016): to define a threshold for automated sound classification. Other potential avenues of analysis are thinkable, e.g. to use the ratio of peak to background in the power spectra for automated detection. The analysis presented here used only the direct result of the spectral analysis for (manual) signal detection, automated signal detection could also make use of the fact that pulsation of seismic airgun signals occurs coherently for a certain width of acoustic frequencies. In relation to power spectra of spectrograms this means to find ways to use the a-priori knowledge of the vertical bar structure of pulsating signals, even if their exact position and extent is not a-priori known.

Last but not least seismic airgun shots are not the only known example of regularly pulsating anthropogenic noise signatures. Ship cavitation noise is another possible example. As reported in Geyer et al. (2016)¹, the recorded cavitation noise from the involved research icebreaker, characterized by its ringing sound, with a modulation period of about 4.5 Hz. Given high enough sampling frequencies of the original recording, power spectra of spectrograms can be possible means of analysis for this and other sound types as well.

4 REFERENCES

1. F. Geyer, H. Sagen, G. Hope, M. Babiber and P. F. Worcester, Identification and quantification of soundscape components in the Marginal Ice Zone, *J. Acoust. Soc. Am.* 139 (4), 1873-1885 (2016).